

# Arrangement of a NO ligand and the neighboring sulfur-containing species on a dinuclear ruthenium complex by ligand substitution and linkage isomerism of a dimethyl sulfoxide ligand

Yasuhiro Arikawa,\* Yuji Otsubo, Tomofumi Nakayama, Naoto Mitsuda, Shinnosuke Horiuchi, Eri Sakuda, and Keisuke Umakoshi

*Division of Chemistry and Materials Science, Graduate School of Engineering, Nagasaki University, Bunkyo-machi 1-14, Nagasaki 852-8521, Japan.*

Received January \*\*, 2019

## Abstract

The substitution reactions of a NO-ligated dinuclear ruthenium complex with ammonium thiocyanate (NH<sub>4</sub>SCN), sulfur, and dimethyl sulfoxide (DMSO) gave the corresponding mononitrosyl dinuclear complexes, except for reaction with sulfur, where diastereomers of a S<sub>2</sub>-bridged tetranuclear complex along with a NO- and S<sub>2</sub>-bridged dinuclear complex were obtained. According to the scan rate dependent cyclic voltammograms, linkage isomerism of a dmsoligand on the dinuclear complex was revealed, and the linkage isomer was obtained from the chemical oxidation.

*Keywords:* Substitution Reaction; Linkage isomerism; Sulfur; Dinuclear; Ruthenium.

\*Corresponding author. Tel./fax: +81 95 819 2673

*E-mail address:* arikawa@nagasaki-u.ac.jp (Y. Arikawa)

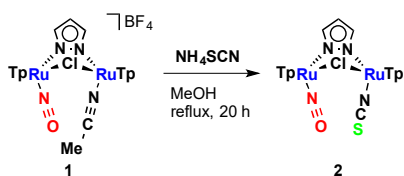
## 1. Introduction

Metal nitrosyl complexes became a subject of particular interest due to their biological relevance such as vasodilation [1], nitrosative stress [2] in immune response, and bacterial NO reductase (NOR) [3]. In relation to the NOR, we found an unusual N–N coupling of two NO ligands on a dinuclear ruthenium complex as a key part [4a]. The use of the N–N coupling complex achieved a NO reduction cycle ( $2\text{NO} + 2\text{H}^+ + 2\text{e}^- \rightarrow \text{N}_2\text{O} + \text{H}_2\text{O}$ ) [4]. Recently, on the same dinuclear ruthenium platform  $\{(\text{TpRu})_2(\mu\text{-pz})\}$  (Tp = HB(pyrazol-1-yl)<sub>3</sub>), a synthetic nitrite reduction cycle ( $\text{NO}_2^- + 7\text{H}^+ + 6\text{e}^- \rightarrow \text{NH}_3 + 2\text{H}_2\text{O}$ ) could be achieved [5]. The cycle

comprises conversion of a nitrito ligand to a NO ligand using  $2\text{H}^+$  and  $\text{e}^-$ , subsequent reduction of the NO ligand to a nitrido and a  $\text{H}_2\text{O}$  ligand by consumption of  $2\text{H}^+$  and  $5\text{e}^-$ , and recovery of the parent nitrito ligand releasing ammonia. In the cycle, a curious bent-type nitrido-bridged dinuclear complex was isolated. The clue of this findings includes the substitution reaction of  $[\{\text{TpRu}(\text{NCMe})\}\{\text{TpRu}(\text{NO})\}(\mu\text{-Cl})(\mu\text{-pz})]\text{BF}_4$  (**1**) with pyridine *N*-oxide, followed by N–O coupling liberating the pyridine. This prompted us to check the substitution reaction of **1** with sulfur and sulfur-containing species, although we have already reported the substitution with NO [6]. In this paper, we report the reactions of **1** with ammonium thiocyanate ( $\text{NH}_4\text{SCN}$ ), sulfur, and dimethyl sulfoxide (DMSO). The linkage isomerism on the dinuclear ruthenium complex is also observed.

## 2. Results and Discussion

The substitution reaction of  $[\{\text{TpRu}(\text{NCMe})\}\{\text{TpRu}(\text{NO})\}(\mu\text{-Cl})(\mu\text{-pz})]\text{BF}_4$  (**1**) with  $\text{NH}_4\text{SCN}$  in MeOH heated to reflux for 20 h afforded a *N*-bonded thiocyanato complex  $[\{\text{TpRu}(\text{NCS})\}\{\text{TpRu}(\text{NO})\}(\mu\text{-Cl})(\mu\text{-pz})]$  (**2**) in 91% yield (Scheme 1). The  $^1\text{H}$  NMR spectrum of **2** shows diamagnetic signals assignable to seven distinct sets of peaks of the pyrazolyl groups (two Tp and one bridging pyrazolyl ligands), indicating retention of the unsymmetrical dinuclear complex. The presence of the NCS and NO ligands is proved by the IR spectrum ( $\nu(\text{CN})$  2097 (s) and  $\nu(\text{NO})$  1876 (s)  $\text{cm}^{-1}$ ). From the cationic nature of the NO ligand and the diamagnetic nature of **2**, the oxidation states of two ruthenium centers would be II. The FAB-MS spectrum shows the signal of the molecular ion at  $m/z$  819.1 as well as signals at  $m/z$  789.1 and 761.1 due to loss of a NO and a NCS ligand, respectively. The structure is finally confirmed by the X-ray crystallographic analysis (Fig. 1). The structure is a neutral dinuclear complex bridged by a chlorido and a pyrazolato ligand, and each ruthenium is coordinated by a NO and a *N*-bonded thiocyanate ligand, respectively. The N–O bond distance of **2** (1.139(2) Å) is almost unchanged as compared to that of **1** (1.145(12) Å) (Table 1). The N–C and C–S bond distances are 1.159(3) and 1.655(2) Å, respectively, which are similar to those of other TpRu complexes,  $[\text{TpRu}(\text{NCS})(\text{CN}^t\text{Bu})_2]$  [7] and  $[\text{TpRu}(\text{NCS})(\text{PPh}_3)(\text{PTA})]$  (PTA = 1,3,5-triaza-7-phosphaadamantane) [8]. The *N*-bonded thiocyanate group displays a linear NCS arrangement (Ru–N–C and N–C–S angles;  $165.65(17)^\circ$  and  $179.1(2)^\circ$ , respectively). The linkage isomer (*S*-bonded thiocyanate ligated complex) was not observed, probably due to steric hindrance of a *S*-bonded thiocyanate ligand, which coordinates to the metal center in a bent form [9].



**Scheme 1.** Substitution reaction of **1** with  $\text{NH}_4\text{SCN}$ .

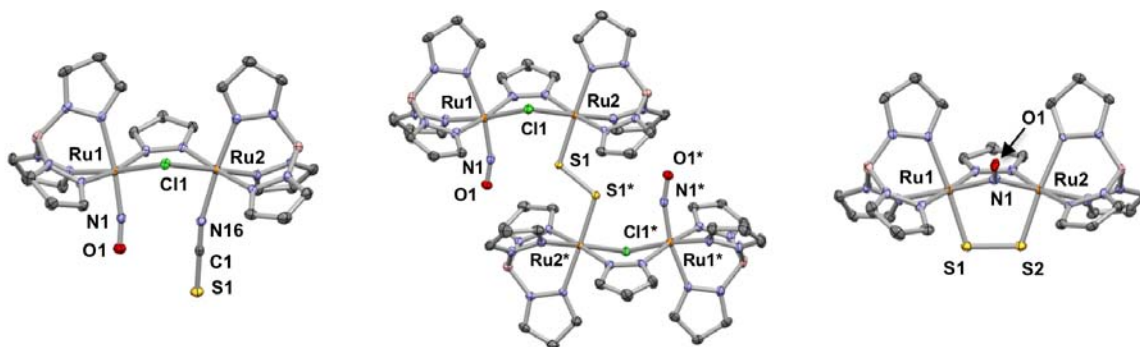
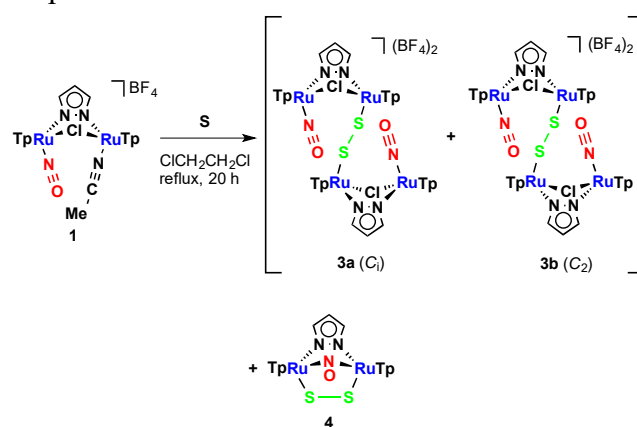


**Fig. 1.** Structures of **2** (left) and **4** (right) and the cation part of **3a** (center), with ellipsoids drawn at the 50% probability level. The counter  $\text{BF}_4$  ions of **3a**, crystallization solvents, and hydrogen atoms are omitted for clarity. Selected bond lengths (Å) and angles ( $^\circ$ ) are as follows. For **2**: Ru(1)–N(1) 1.7625(18), Ru(2)–N(16) 2.0395(18), S(1)–C(1) 1.655(2), N(16)–C(1) 1.159(3), O(1)–N(1) 1.139(2); Ru(1)–N(1)–O(1) 169.57(17), Ru(2)–N(16)–C(1) 165.65(17), S(1)–C(1)–N(16) 179.1(2). For **3a**: Ru(1)–N(1) 1.764(3), Ru(2)–S(1) 2.2040(10), S(1)–S(1\*) 1.9761(13), O(1)–N(1) 1.145(4); Ru(1)–N(1)–O(1) 163.1(3), Ru(2)–S(1)–S(1\*) 111.22(5). For **4**: Ru(1)–S(1) 2.213(2), Ru(2)–S(2) 2.212(2), Ru(1)–N(1) 1.968(6), Ru(2)–N(1) 1.978(6), S(1)–S(2) 2.004(3), O(1)–N(1) 1.240(7); Ru(1)–S(1)–S(2) 108.41(10), Ru(2)–S(2)–S(1) 107.34(10), Ru(1)–N(1)–Ru(2) 116.9(3).

(Table 1 here)

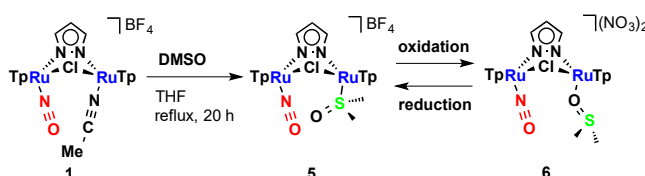
Reactions of  $[\{\text{TpRu}(\text{NCMe})\}\{\text{TpRu}(\text{NO})\}(\mu\text{-Cl})(\mu\text{-pz})]\text{BF}_4$  (**1**) with sulfur in refluxing  $\text{ClCH}_2\text{CH}_2\text{Cl}$  for 20 h gave two types of disulfide complexes,  $[\{(\text{TpRu}(\text{NO}))(\text{TpRu})(\mu\text{-Cl})(\mu\text{-pz})\}_2(\mu\text{-S}_2)](\text{BF}_4)_2$  (**3**) (51% yield) and  $[(\text{TpRu})_2(\mu\text{-NO})(\mu\text{-pz})(\mu\text{-S}_2)]$  (**4**) (18% yield) after column-chromatographic separation (Scheme 2). The  $^1\text{H}$  NMR spectrum of **4** shows diamagnetic signals assignable to four distinct sets of peaks of the pyrazolyl groups (Tp and bridging pyrazolyl ligands), indicating their  $C_s$  symmetry. The IR spectrum of **4** exhibits the disappearance of  $\nu(\text{N}\equiv\text{O})$  stretching band. The structure of **4** was revealed by the X-ray crystallographic analysis (Fig. 1). Two TpRu fragments are bridged by a pyrazolato, NO, and an end-on *cis*- $\text{S}_2$  ligand. The N–O distance (1.240(7) Å) is similar to that of  $[(\text{TpRu})_2(\mu\text{-Cl})(\mu\text{-NO})(\mu\text{-pz})]$  (1.209(5) Å) [6]. The S–S distance is 2.004(3) Å is slightly longer than those of similar chlorido- and disulfide-bridged dinuclear ruthenium complexes (av. 1.972 Å) [10]. The formation mechanism of **4** is unclear. In contrast to **4**, the FAB-MS spectrum of **3** exhibits

peaks assignable to a tetranuclear complex and the  $^1\text{H}$  NMR shows complicated signals, but indicates presence of two species, diastereomers (**3a** and **3b**) with an approximate ratio of 1:1. Unfortunately, we failed to separate the diastereomers, but single crystals of one of the diastereomers (**3a**) were obtained by chance. Structure of the cation part of **3a** is shown in Fig. 1. Two dinuclear fragments  $\{(\text{TpRu}(\text{NO}))(\text{TpRu})(\mu\text{-Cl})(\mu\text{-pz})\}$  are bridged by an end-on *trans*- $\text{S}_2$  ligand in a  $C_i$  symmetry manner. The dinuclear complex **1** is a chiral complex, thus connecting of the two dinuclear parts through  $\text{S}_2$ , leading to the tetranuclear complex, results in diastereomers. The other (**3b**) should have  $C_2$  symmetry. The S–S distance (1.9761(13) Å) is comparable to the corresponding one in a similar  $(\text{TpRu})_2(\mu\text{-S}_2)$  complex (1.987(2) Å) [11]. To proceed with the S–S bond cleavage of **3**, reduction reaction of **3** was carried out. However, we obtained unidentified products.



**Scheme 2.** Substitution reaction of **1** with sulfur.

Lastly, the substitution reaction of  $\{[\text{TpRu}(\text{NCMe})]\{[\text{TpRu}(\text{NO})](\mu\text{-Cl})(\mu\text{-pz})\}\text{BF}_4$  (**1**) with DMSO in THF under reflux for 20 h resulted in a *S*-bounded dmsso complex  $\{[\text{TpRu}(\text{dmsso-}\kappa\text{S})]\{[\text{TpRu}(\text{NO})](\mu\text{-Cl})(\mu\text{-pz})\}\text{BF}_4$  (**5**) in 85% yield (Scheme 3). The MeCN ligand is smoothly exchanged by dmsso, and the structure of **5** was characterized by IR, NMR, and ESI-MS spectroscopy and X-ray crystallographically confirmed (Fig. 2). The bond distance between ruthenium and sulfur (2.228(2) Å) is similar to that of  $[\text{TpRuCl}(\text{dmsso})_2]$  (2.288(1) and 2.250(1) Å) [12].



**Scheme 3.** Substitution reaction of **1** with DMSO and linkage isomerism of a dmsso ligand.

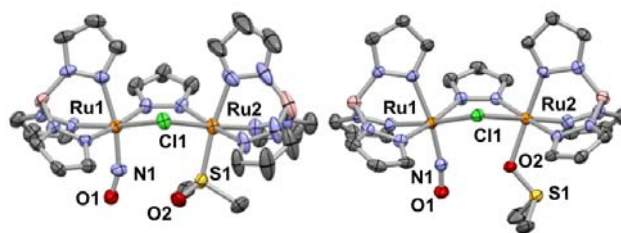


**Fig. 2.** Structures of the cation part of **5** (left) and **6** (right), with ellipsoids drawn at the 50% probability level. The counter ions, crystallization solvents, and hydrogen atoms are omitted for clarity. Selected bond lengths (Å) and angles (°) are as follows. For **5**: Ru(1)–N(1) 1.767(6), Ru(2)–S(1) 2.228(2), S(1)–O(2) 1.490(6), O(1)–N(1) 1.139(9); Ru(1)–N(1)–O(1) 161.0(6), Ru(2)–S(1)–O(2) 118.4(3). For **6**: Ru(1)–N(1) 1.763(4), Ru(2)–O(2) 2.056(3), S(1)–O(2) 1.559(3), O(1)–N(1) 1.140(5); Ru(1)–N(1)–O(1) 168.3(4), Ru(2)–O(2)–S(1) 121.16(19).

The linkage isomerism of the dmsol complex was recognized by cyclic voltammetry (CV) experiments. The voltammogram of **5** in CH<sub>2</sub>Cl<sub>2</sub>, starting at 0 V at different scan rates, is shown in Fig. 3. In the scan rate of 0.05 V/s (Figure 3(a)), an irreversible anodic wave at  $E_{pa} = 1.22$  V (vs. Ag/AgCl) and an irreversible cathodic wave at  $E_{pc} = 0.36$  V (vs. Ag/AgCl) can be seen. On the other hand, at 1.0 V/s scan rate (Figure 3(b)), additional cathodic wave at  $E_{pc} = 1.09$  V (vs. Ag/AgCl) appeared, resulting in one quasi-reversible wave ( $E_{1/2} = 1.16$  V (vs. Ag/AgCl)). This is the typical behavior associated with a DMSO linkage isomerism [13]. At faster scan rate, the redox process for Ru(III)/Ru(II) couple, where DMSO is bonded through the S atom, can be observed. At slower scan rate, this process is irreversible and this behaviour can be attributed to a relatively fast linkage isomerization of the dmsol ligand in the oxidized species forming Ru<sup>III</sup>(dmsol-κO) (Scheme 4). The harder Ru(III) Lewis acid would prefer O-ligation of a dmsol ligand, consistent with the hard-soft acid-base theory (HSAB). The Ru<sup>III</sup>(dmsol-κO) species would be irreversibly reduced to **5** at  $E_{pa} = 0.36$  V. This observation motivated us to isolate the oxidized species by the chemical oxidation.

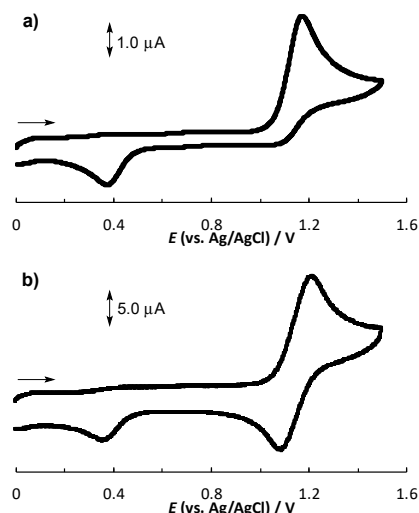
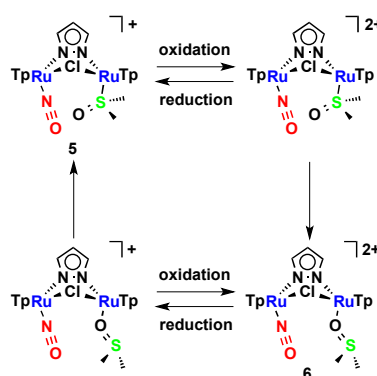


**Fig. 3.** Cyclic voltammograms of **5** (0.1 mM) in CH<sub>2</sub>Cl<sub>2</sub> containing <sup>n</sup>Bu<sub>4</sub>NPF<sub>6</sub> (0.1 M) starting the scanning at  $E = 0$  V; working electrode: Pt; counter electrode: Pt; reference: Ag/AgCl; scan rate: (a) 0.05 V s<sup>-1</sup>, (b) 1.0 V s<sup>-1</sup>.



**Scheme 4.** Linkage isomerization processes of a dmsO complex.

Treatment of [ $\{\text{TpRu}(\text{dmsO}-\kappa\text{S})\}\{\text{TpRu}(\text{NO})\}(\mu\text{-Cl})(\mu\text{-pz})\}\text{BF}_4$  (**5**) with  $(\text{NH}_4)_2[\text{Ce}(\text{NO}_3)_6]$  in MeOH for 3 h at room temperature afforded [ $\{\text{TpRu}(\text{dmsO}-\kappa\text{O})\}\{\text{TpRu}(\text{NO})\}(\mu\text{-Cl})(\mu\text{-pz})\}(\text{NO}_3)_2$  (**6**) in 89% yield (Scheme 3). The paramagnetic complex **6** was confirmed by the X-ray crystallographic analysis (Fig. 2). The asymmetric unit includes two crystallographically independent molecules of **6**. The dmsO ligands are coordinated to the ruthenium atom through the O atom instead of the S atom. The ruthenium–oxygen bond distances are 2.056(3) and 2.051(5) Å, and the S–O bond distances of the dmsO ligands (1.559(3) and 1.544(6) Å) are longer than that of **5** (1.490(6) Å). Chemical reduction of **6** with  $[\text{Cp}^*_2\text{Fe}]$  afforded [ $\{\text{TpRu}(\text{dmsO}-\kappa\text{S})\}\{\text{TpRu}(\text{NO})\}(\mu\text{-Cl})(\mu\text{-pz})\}]^+$ , indicating the reversibility. In the dinuclear complex, oxidation would occur at one of two ruthenium atoms ( $\text{Ru}(\text{dmsO}-\kappa\text{S})$ ). Because the other ruthenium atom is difficult to be oxidized due to the ligation of the strong electron withdrawing  $\text{NO}^+$ . We performed the CV experiments of **5** to +2.0 V, but the second oxidation

process was not observed. Other unsymmetrical mononitrosyl dinuclear ruthenium complexes [14] and the neutral complex **2**, which is expected to be oxidized easier than the cationic complex **5**, don't show also the second oxidation process in the CV experiments.

### 3. Conclusion

Use of the versatile complex **1**, through the substitution reaction for a MeCN ligand, gave the NCS-ligated complex **2**, diastereomers of the S<sub>2</sub>-bridged tetranuclear complexes (**3a** and **3b**) along with the S<sub>2</sub>-bridged dinuclear complex **4**, and the dmsoligated complex **5**. Although the linkage isomerization of **2** was not detected, the scan rate dependent cyclic voltammograms showed the isomerism of the dmsoligand of **5**. Moreover, the linkage isomer **6** was obtained from the chemical oxidation. All new complexes except for one of the diastereomers (**3b**) were characterized by the X-ray crystallographic analyses.

### 4. Experimental

#### 4.1. General

All reactions were carried out under N<sub>2</sub> or Ar unless otherwise noted, and subsequent work-up manipulations were performed in air. The starting complex [ $\{\text{TpRu}(\text{NCMe})\}\{\text{TpRu}(\text{NO})\}(\mu\text{-Cl})(\mu\text{-pz})\text{]BF}_4$  (**1**) was prepared according to the previously reported method [6]. Organic solvents and all other reagents were commercially available and used without further purification. NMR spectra were recorded on a Varian Gemini-300 and a JEOL JNM-AL-400 spectrometer. <sup>1</sup>H and <sup>13</sup>C{<sup>1</sup>H} NMR chemical shifts are quoted with respect to tetramethylsilane and the solvent signals, respectively. Infrared spectra in KBr pellets were obtained on a JASCO FT-IR-4100 spectrometer. Fast atom bombardment mass spectra (FAB-MS) and electrospray mass spectra (ESI-MS) were carried out on a JEOL JMS-700N and a Waters ACQUITY SQD MS system, respectively. Elemental analyses (C, H, N) were performed on a PerkinElmer 2400II elemental analyzer. Cyclic voltammetry was recorded at room temperature with a BAS ALS-600C electrochemical analyzer by using a platinum disk working electrode, a platinum wire counter electrode, and a Ag/AgCl reference electrode. Cyclic voltammograms were recorded for 1.0 mM test solutions of the complexes with 0.1 M [<sup>n</sup>Bu<sub>4</sub>N][PF<sub>6</sub>] as a supporting electrolyte.

#### 4.2. Preparation of [ $\{\text{TpRu}(\text{NCS})\}\{\text{TpRu}(\text{NO})\}(\mu\text{-Cl})(\mu\text{-pz})$ ] (**2**)

A mixture of [ $\{\text{TpRu}(\text{NCMe})\}\{\text{TpRu}(\text{NO})\}(\mu\text{-Cl})(\mu\text{-pz})\text{]BF}_4$  (**1**) (45 mg, 0.051 mmol) and

NH<sub>4</sub>SCN (13 mg, 0.17 mmol) in MeOH (15 mL) was refluxed for 20 h. After evaporation to dryness, the residue was column-chromatographed with a silica gel eluting with CH<sub>2</sub>Cl<sub>2</sub>-acetone (25/1) to afford [ $\{\text{TpRu}(\text{NCS})\}\{\text{TpRu}(\text{NO})\}(\mu\text{-Cl})(\mu\text{-pz})$ ] (**2**) (37.8 mg, 91%) as green powder. IR (KBr, pellet):  $\nu(\text{BH})$  2477 (w),  $\nu(\text{CN})$  2097 (s),  $\nu(\text{NO})$  1876 (s) cm<sup>-1</sup>. <sup>1</sup>H NMR (CDCl<sub>3</sub>):  $\delta$  8.11 (d,  $J = 2.2$  Hz, 1H, pz), 8.02 (d,  $J = 1.5$  Hz, 1H, pz), 8.00 (d,  $J = 2.2$  Hz, 1H, pz), 7.97 (d,  $J = 2.5$  Hz, 1H, pz), 7.89 (d,  $J = 2.5$  Hz, 1H, pz), 7.75 (d,  $J = 2.3$  Hz, 1H x 2, pz), 7.72 (d,  $J = 2.0$  Hz, 1H x 2, pz), 7.64 (d,  $J = 1.9$  Hz, 1H, pz), 7.07 (d,  $J = 1.9$  Hz, 1H, pz), 7.02 (d,  $J = 2.2$  Hz, 1H, pz), 6.87 (d,  $J = 2.3$  Hz, 1H, pz), 6.84 (d,  $J = 1.5$  Hz, 1H, pz), 6.62 (t,  $J = 2.4$  Hz, 1H, 4-pz), 6.53 (t,  $J = 2.3$  Hz, 1H, 4-pz), 6.27 (t,  $J = 2.2$  Hz, 1H x 2, 4-pz), 6.23 (t,  $J = 2.1$  Hz, 1H, 4-pz), 6.16 (t,  $J = 2.0$  Hz, 1H, 4-pz), 6.11 (t,  $J = 1.9$  Hz, 1H, 4-pz). <sup>13</sup>C{<sup>1</sup>H} NMR (CDCl<sub>3</sub>):  $\delta$  144.9 (pz), 144.2 (pz x 2), 143.9 (pz), 143.6 (pz), 143.0 (pz), 142.8 (pz), 141.0 (pz), 137.6 (pz), 137.2 (pz), 136.1 (pz), 135.5 (pz), 135.1 (pz), 135.0 (pz), 108.9 (4-pz), 108.2 (4-pz), 107.1 (4-pz), 106.7 (4-pz), 106.3 (4-pz), 105.6 (4-pz), 105.1 (4-pz). FAB-MS ( $m/z$ ): 819.1 [M]<sup>+</sup>, 789.1 [M-(NO)]<sup>+</sup>, 761.1 [M-(NCS)]<sup>+</sup>. Elemental analysis(%) calcd for C<sub>22</sub>H<sub>23</sub>N<sub>16</sub>B<sub>2</sub>ClORu<sub>2</sub>S: C, 32.27; H, 2.83; N, 27.37; found: C, 32.97; H, 2.83; N, 26.81.

#### 4.3. Reaction of [ $\{\text{TpRu}(\text{NCMe})\}\{\text{TpRu}(\text{NO})\}(\mu\text{-Cl})(\mu\text{-pz})$ ] $\text{BF}_4$ (**1**) with sulfur

A mixture of [ $\{\text{TpRu}(\text{NCMe})\}\{\text{TpRu}(\text{NO})\}(\mu\text{-Cl})(\mu\text{-pz})$ ] $\text{BF}_4$  (**1**) (30 mg, 0.034 mmol) and sulfur (6.0 mg, 0.19 mmol) in ClCH<sub>2</sub>CH<sub>2</sub>Cl (10 mL) was refluxed for 20 h. The solution was dried *in vacuo*, and the residue was column-chromatographed with a silica gel eluting with CH<sub>2</sub>Cl<sub>2</sub> to afford [(TpRu)<sub>2</sub>( $\mu\text{-NO}$ )( $\mu\text{-pz}$ )( $\mu\text{-S}_2$ )] (**4**) (4.8 mg, 18%) as red-purple powder. The use of CH<sub>2</sub>Cl<sub>2</sub>-acetone (5/1) as an eluent led to [ $\{(\text{TpRu}(\text{NO}))(\text{TpRu})(\mu\text{-Cl})(\mu\text{-pz})\}_2(\mu\text{-S}_2)$ ](BF<sub>4</sub>)<sub>2</sub> (**3**) as green powder (15.2 mg, 51%). **Complex 3**: IR (KBr, pellet):  $\nu(\text{BH})$  2517 (m),  $\nu(\text{NO})$  1878 (s),  $\nu(\text{BF})$  1120–1053 (s) cm<sup>-1</sup>. <sup>1</sup>H NMR (CD<sub>3</sub>CN):  $\delta$  8.24 (d,  $J = 2.0$  Hz, 1H, pz), 8.22 (d,  $J = 2.2$  Hz, 1H x 3, pz), 8.12 (d,  $J = 2.3$  Hz, 1H x 2, pz), 8.07 (d,  $J = 1.9$  Hz, 1H, pz), 8.00–7.98 (m, 1H x 4, pz), 7.96 (d,  $J = 1.9$  Hz, 1H, pz), 7.85 (d,  $J = 1.9$  Hz, 1H, pz), 7.77 (d,  $J = 1.8$  Hz, 1H, pz), 7.70 (d,  $J = 2.3$  Hz, 1H, pz), 7.68 (d,  $J = 2.0$  Hz, 1H, pz), 7.41 (d,  $J = 1.9$  Hz, 1H, pz), 7.28 (d,  $J = 1.9$  Hz, 1H, pz), 7.18 (d,  $J = 2.1$  Hz, 1H, pz), 7.17 (d,  $J = 2.1$  Hz, 1H, pz), 7.08 (d,  $J = 2.1$  Hz, 1H, pz), 6.96 (d,  $J = 2.2$  Hz, 1H, pz), 6.81 (d,  $J = 1.6$  Hz, 1H, pz), 6.77 (t,  $J = 2.5$  Hz, 1H, 4-pz), 6.75 (t,  $J = 2.5$  Hz, 1H, 4-pz), 6.66–6.65 (m, 1H x 2, pz), 6.64 (t,  $J = 2.4$  Hz, 1H, 4-pz), 6.55 (t,  $J = 2.5$  Hz, 1H, 4-pz), 6.54 (t,  $J = 2.6$  Hz, 1H, 4-pz), 6.53 (t,  $J = 2.4$  Hz, 1H, 4-pz), 6.52 (t,  $J = 2.4$  Hz, 1H, 4-pz), 6.48 (d,  $J = 1.6$  Hz, 1H, pz), 6.38 (t,  $J = 2.4$  Hz, 1H, 4-pz), 6.38 (t,  $J = 2.4$  Hz, 1H, 4-pz), 6.30 (t,  $J = 2.3$  Hz, 1H, 4-pz), 6.24–6.22 (m, 1H x 3, pz), 6.20 (t,  $J = 2.4$  Hz, 1H, 4-pz), 6.07 (d,  $J = 1.7$  Hz, 1H x 2, pz). FAB-MS ( $m/z$ ): 1673.1 [M+BF<sub>4</sub>]<sup>+</sup>, 1586.1 [M]<sup>+</sup>, 793.0 [ $\{(\text{TpRu}(\text{NO}))(\text{TpRu})(\mu\text{-Cl})(\mu\text{-pz})\}\text{S}$ ]<sup>+</sup>, 761.1 [ $\{(\text{TpRu}(\text{NO}))(\text{TpRu})(\mu\text{-Cl})(\mu\text{-pz})\}$ ]<sup>+</sup>. Elemental analysis(%) calcd for C<sub>42</sub>H<sub>46</sub>N<sub>30</sub>B<sub>6</sub>Cl<sub>2</sub>F<sub>8</sub>O<sub>2</sub>Ru<sub>4</sub>S<sub>2</sub>: C, 28.68; H, 2.64;

N, 23.89; found: C, 28.18; H, 2.77; N, 23.73. **Complex 4:** IR (KBr, pellet):  $\nu(\text{BH})$  2481 (m),  $\nu(\text{NO})$  1483 (m)  $\text{cm}^{-1}$ .  $^1\text{H}$  NMR ( $\text{CDCl}_3$ ):  $\delta$  7.95 (d,  $J = 2.4$  Hz, 2H, pz), 7.83 (d,  $J = 2.3$  Hz, 2H, pz), 7.73 (d,  $J = 2.4$  Hz, 2H, pz), 7.54 (d,  $J = 2.0$  Hz, 2H, pz), 6.77 (d,  $J = 1.9$  Hz, 2H, pz), 6.43 (t,  $J = 2.1$  Hz, 2H, 4-pz), 6.40 (d,  $J = 2.1$  Hz, 2H, pz), 6.19 (t,  $J = 2.1$  Hz, 2H, 4-pz), 6.10 (d,  $J = 2.0$  Hz, 2H, pz), 6.05 (t,  $J = 2.1$  Hz, 2H, 4-pz), 5.98 (t,  $J = 2.0$  Hz, 1H, 4-pz).  $^{13}\text{C}\{^1\text{H}\}$  NMR ( $\text{CDCl}_3$ ):  $\delta$  145.1 (pz), 143.4 (pz), 142.9 (pz), 140.0 (pz), 136.7 (pz), 135.3 (pz), 135.2 (pz), 106.9 (4-pz), 106.6 (4-pz), 105.9 (4-pz), 105.4 (4-pz). FAB-MS ( $m/z$ ): 790.1 ( $[\text{M}]^+$ ), 759.1 ( $[\text{M}-\text{S}+1]^+$ ). Elemental analysis (%) calcd. for  $\text{C}_{21}\text{H}_{23}\text{N}_{15}\text{B}_2\text{ORu}_2\text{S}_2 \cdot \text{CH}_2\text{Cl}_2$ : C 30.22, H 2.88, N 24.03; found: C 30.76, H 3.11, N, 23.86.

#### 4.4. Preparation of [ $\{\text{TpRu}(\text{dmsO}-\kappa\text{S})\}\{\text{TpRu}(\text{NO})\}(\mu\text{-Cl})(\mu\text{-pz})\text{BF}_4$ ] (**5**)

DMSO (30 mg, 0.38 mmol) was added to a THF (15 mL) solution of [ $\{\text{TpRu}(\text{NCMe})\}\{\text{TpRu}(\text{NO})\}(\mu\text{-Cl})(\mu\text{-pz})\text{BF}_4$ ] (**1**) (60 mg, 0.068 mmol). The mixture was refluxed for 20 h, during this time the solution turned to dark green. After evaporation to dryness, the residue was column-chromatographed with a silica gel eluting with  $\text{CH}_2\text{Cl}_2$ -acetone (5/1) to afford [ $\{\text{TpRu}(\text{dmsO}-\kappa\text{S})\}\{\text{TpRu}(\text{NO})\}(\mu\text{-Cl})(\mu\text{-pz})\text{BF}_4$ ] (**5**) (53.2 mg, 85%) as green powder. IR (KBr, pellet):  $\nu(\text{BH})$  2520 (m),  $\nu(\text{NO})$  1888 (s),  $\nu(\text{BF})$  1121–1053 (s)  $\text{cm}^{-1}$ .  $^1\text{H}$  NMR ( $\text{CDCl}_3$ ):  $\delta$  8.32 (d,  $J = 2.2$  Hz, 1H, pz), 8.16 (d,  $J = 1.6$  Hz, 1H, pz), 8.11 (d,  $J = 1.9$  Hz, 1H, pz), 8.03 (d,  $J = 2.3$  Hz, 1H, pz), 7.97 (d,  $J = 2.1$  Hz, 1H, pz), 7.90 (d,  $J = 2.3$  Hz, 1H, pz), 7.86 (d,  $J = 1.9$  Hz, 1H, pz), 7.84 (d,  $J = 2.1$  Hz, 1H, pz), 7.78 (d,  $J = 2.1$  Hz, 1H, pz), 7.47 (d,  $J = 1.8$  Hz, 1H, pz), 7.36 (d,  $J = 1.9$  Hz, 1H, pz), 7.29 (d,  $J = 2.3$  Hz, 1H, pz), 7.17 (d,  $J = 1.8$  Hz, 1H, pz), 6.69 (t,  $J = 2.4$  Hz, 1H, 4-pz), 6.64 (d,  $J = 2.2$  Hz, 1H, pz), 6.52 (t,  $J = 2.4$  Hz, 1H, 4-pz), 6.42 (t,  $J = 2.3$  Hz, 1H, 4-pz), 6.37 (t,  $J = 2.2$  Hz, 1H, 4-pz), 6.35 (t,  $J = 2.3$  Hz, 1H, 4-pz), 6.24 (t,  $J = 2.4$  Hz, 1H, 4-pz), 6.20 (t,  $J = 2.2$  Hz, 1H, 4-pz), 3.17 (s, 3H,  $\text{CH}_3$ ), 2.31 (s, 3H,  $\text{CH}_3$ ).  $^{13}\text{C}\{^1\text{H}\}$  NMR ( $\text{CDCl}_3$ ):  $\delta$  145.4 (pz), 144.9 (pz), 144.4 (pz), 144.3 (pz), 144.2 (pz), 143.7 (pz), 142.6 (pz), 142.1 (pz), 138.4 (pz), 137.8 (pz x 2), 137.2 (pz), 136.6 (pz), 136.2 (pz), 109.8 (4-pz), 109.0 (4-pz), 108.5 (4-pz), 107.8 (4-pz), 106.9 (4-pz), 106.8 (4-pz), 106.0 (4-pz), 45.8 (Me), 44.2 (Me). ESI-MS ( $m/z$ ): 839.0  $[\text{M}]^+$ . Elemental analysis (%) calcd for  $\text{C}_{23}\text{H}_{29}\text{N}_{15}\text{B}_3\text{ClF}_4\text{O}_2\text{Ru}_2\text{S}$ : C, 29.84; H, 3.16; N, 22.70; found: C, 29.98; H, 3.20; N, 22.47.

#### 4.5. Preparation of [ $\{\text{TpRu}(\text{dmsO}-\kappa\text{O})\}\{\text{TpRu}(\text{NO})\}(\mu\text{-Cl})(\mu\text{-pz})\text{NO}_3$ ] (**6**)

A mixture of [ $\{\text{TpRu}(\text{dmsO}-\kappa\text{S})\}\{\text{TpRu}(\text{NO})\}(\mu\text{-Cl})(\mu\text{-pz})\text{BF}_4$ ] (**5**) (22.1 mg, 0.024 mmol) and  $(\text{NH}_4)_2[\text{Ce}(\text{NO}_3)_6]$  (14.7 mg, 0.027 mmol) in MeOH (5 mL) was stirred for 3 h at room temperature. The solution was dried *in vacuo* and the residue was extracted with  $\text{CH}_2\text{Cl}_2$  to afford [ $\{\text{TpRu}(\text{dmsO}-\kappa\text{O})\}\{\text{TpRu}(\text{NO})\}(\mu\text{-Cl})(\mu\text{-pz})\text{NO}_3$ ] (**6**) as an orange solid (20.5 mg, 89%). IR (KBr, pellet):  $\nu(\text{BH})$  2528 (w),  $\nu(\text{NO})$  1914 (s)  $\text{cm}^{-1}$ . ESI-MS ( $m/z$ ): 839.0  $[\text{M}]^+$ ,

419.6 [M]<sup>2+</sup>. Elemental analysis(%) calcd for C<sub>23</sub>H<sub>29</sub>N<sub>17</sub>B<sub>2</sub>ClO<sub>8</sub>Ru<sub>2</sub>S·H<sub>2</sub>O: C, 28.16; H, 3.19; N, 24.28; found: 28.28; H, 2.91; N, 23.79.

#### 4.6. Reaction of [*TPRu(dmsO-κO)*]*TPRu(NO)*(μ-Cl)(μ-pz)](NO<sub>3</sub>)<sub>2</sub> (**6**) with [*Cp*\*<sub>2</sub>Fe]

A mixture of [*TPRu(dmsO-κO)*]*TPRu(NO)*(μ-Cl)(μ-pz)](NO<sub>3</sub>)<sub>2</sub> (**6**) (28.2 mg, 0.029 mmol) and [*Cp*\*<sub>2</sub>Fe] (11.4 mg, 0.035 mmol) in MeOH (5 mL) was stirred for 3 h at room temperature. After evaporation to dryness, the residue was column-chromatographed with a silica gel eluting with CH<sub>2</sub>Cl<sub>2</sub>-acetone (2/1) to afford [*TPRu(dmsO-κS)*]*TPRu(NO)*(μ-Cl)(μ-pz)]NO<sub>3</sub> (20.0 mg, 77%) as green powder. IR (KBr, pellet): ν(BH) 2479 (w), ν(NO) 1888 (m) cm<sup>-1</sup>. <sup>1</sup>H NMR (CDCl<sub>3</sub>): δ 8.55 (brd, 1H, pz), 8.14 (brd, 2H, pz), 7.97 (brd, 1H, pz), 7.92 (brd, 1H, pz), 7.87 (brd, 1H, pz), 7.84 (brd, 1H, pz), 7.79 (brd, 1H, pz), 7.77 (brd, 1H, pz), 7.50 (brd, 1H, pz), 7.34 (brd, 1H, pz), 7.29 (brd, 1H, pz), 7.15 (brd, 1H, pz), 6.67 (brt, 1H, 4-pz), 6.59 (brd, 1H, pz), 6.50 (brt, 1H, 4-pz), 6.40 (brt, 1H, 4-pz), 6.36 (m, 2H, 4-pz), 6.20 (brt, 1H, 4-pz), 6.17 (brt, 1H, 4-pz), 3.14 (s, 3H, CH<sub>3</sub>), 2.29 (s, 3H, CH<sub>3</sub>). ESI-MS (*m/z*): 839.1 [M]<sup>+</sup>.

#### 4.7. X-ray crystal structural analyses

Crystallographic data are summarized in Table 2. X-ray quality single crystals were obtained from EtOH (for **2**·EtOH), CH<sub>2</sub>Cl<sub>2</sub>/hexane (for **3a**·4MeCN·2H<sub>2</sub>O), (CH<sub>2</sub>Cl<sub>2</sub>+MeCN)/(Me<sub>3</sub>Si)<sub>2</sub>O (for **4**·CH<sub>2</sub>Cl<sub>2</sub>), and MeOH/ether (for **5**·MeOH and **6**·H<sub>2</sub>O). Diffraction data were collected at -180 °C under a stream of cold N<sub>2</sub> gas on a Rigaku RA-Micro7 HFM instrument equipped with a Rigaku Saturn724+ CCD detector by using graphite-monochromated Mo K $\alpha$  radiation. The intensity images were obtained at the exposure of 8.0 s/deg (**2**·EtOH, **5**·MeOH, and **6**·H<sub>2</sub>O), 2.0 s/deg (**3a**·4MeCN·2H<sub>2</sub>O), and 16.0 s/deg (**4**·CH<sub>2</sub>Cl<sub>2</sub>). The frame data were integrated using a Rigaku CrystalClear program package [15], and the data sets were corrected for absorption using a REQAB program [16]. The calculations were performed with a CrystalStructure software package [17]. The structures were solved by direct methods and refined on *F*<sup>2</sup> by the full-matrix least-squares methods. In the asymmetric unit of **6**·H<sub>2</sub>O, there are two crystallographically independent molecules and a H<sub>2</sub>O crystal solvent. One of NO<sub>3</sub><sup>-</sup> anion and the methyl groups in one of dmsO ligands are disordered over two positions with occupancy factors of 0.6/0.4. Moreover, the disordered NO<sub>3</sub><sup>-</sup> anion was restrained. Owing to serious disorder problems of other crystallization solvents, we were not able to define them well. Therefore, a SQUEEZE/PLATON technique was applied. Anisotropic refinement was applied to all non-hydrogen atoms with the exception of H<sub>2</sub>O (**3a**·4MeCN·2H<sub>2</sub>O and **6**·H<sub>2</sub>O) and MeOH (**5**·MeOH) crystal solvents and two NO<sub>3</sub><sup>-</sup> anion. Hydrogen atoms for all structures were put at calculated positions, while those of H<sub>2</sub>O (**3a**·4MeCN·2H<sub>2</sub>O and **6**·H<sub>2</sub>O) and MeOH (**5**·MeOH) crystal solvents and the disordered

methyl groups of dmsoligand ( $6 \cdot \text{H}_2\text{O}$ ) were not included in the calculations.

(Table 2 here)

### Supplementary material

CCDC 1881800 (for  $2 \cdot \text{EtOH}$ ), 1881801 (for  $3\mathbf{a} \cdot 4\text{MeCN} \cdot 2\text{H}_2\text{O}$ ), 1881802 (for  $4 \cdot \text{CH}_2\text{Cl}_2$ ), 1881803 (for  $5 \cdot \text{MeOH}$ ), and 1881804 (for  $6 \cdot \text{H}_2\text{O}$ ) contain the supplementary crystallographic data for this paper. These data can be obtained free of charge from The Cambridge Crystallographic Data Centre via [www.ccdc.cam.ac.uk/data\\_request/cif](http://www.ccdc.cam.ac.uk/data_request/cif).

### Acknowledgements

This work was supported by the JSPS, KAKENHI grant number JP17K05813, and by the priority research project of Nagasaki University. We are grateful to Y. Takeuchi and N. Takemoto at Nagasaki University for their technical assistance.

### References

- [1] (a) M. Follmann, N. Griebenow, M. G. Hahn, I. Hartung, F. J. Mais, J. Mittendorf, M. Schäfer, H. Schirok, J. P. Stasch, F. Stoll, A. Straub, *Angew. Chem. Int. Ed.* **2013**, *52*, 9442-9462;  
(b) E. R. Derbyshire, M. A. Marletta, *Annu. Rev. Biochem.* **2012**, *81*, 533-559;  
(c) T. Shimizu, D. Huang, F. Yan, M. Stranova, M. Bartosova, V. Fojtíková, M. Martínková, *Chem. Rev.* **2015**, *115*, 6491-6533.
- [2] (a) J. D. M. Kurtz, *Dalton Trans.* **2007**, 4115-4121;  
(b) A. M. Gardner, R. A. Helmick, P. R. Gardner, *J. Biol. Chem.* **2002**, *277*, 8172-8177.
- [3] (a) A. M. Wright, T. W. Hayton, *Inorg. Chem.* **2015**, *54*, 9330-9341;  
(b) S. Chakraborty, J. Reed, J. T. Sage, N. C. Branagan, I. D. Petrik, K. D. Miner, M. Y. Hu, J. Zhao, E. E. Alp, Y. Lu, *Inorg. Chem.* **2015**, *54*, 9317-9329;  
(c) A. J. Timmons, M. D. Symes, *Chem. Soc. Rev.* **2015**, *44*, 6708-6722;  
(d) S. Hematian, I. Garcia-Bosch, K. D. Karlin, *Acc. Chem. Res.* **2015**, *48*, 2462-2474;  
(e) T. C. Berto, A. L. Speelman, S. Zheng, N. Lehnert, *Coord. Chem. Rev.* **2013**, *257*, 244-259;  
(f) Y. Shiro, *Biochim. Biophys. Acta* **2012**, *1817*, 1907-1913;  
(g) L. E. Goodrich, F. Paulat, V. K. K. Praneeth, N. Lehnert, *Inorg. Chem.* **2010**, *49*, 6293-6316;

- (h) M. P. Schopfer, J. Wang, K. D. Karlin, *Inorg. Chem.* **2010**, *49*, 6267-6282;
- (i) N. Xu, J. Yi, G. B. Richter-Addo, *Inorg. Chem.* **2010**, *49*, 6253-6266;
- (j) P. Tavares, A. S. Pereira, J. J. G. Moura, I. Moura, *J. Inorg. Biochem.* **2006**, *100*, 2087-2100;
- (k) I. M. Wasser, S. de Vries, P. Moënne-Loccoz, I. Schröder, K. D. Karlin, *Chem. Rev.* **2002**, *102*, 1201-1234;
- (l) B. A. Averill, *Chem. Rev.* **1996**, *96*, 2951-2964.
- [4] (a) Y. Arikawa, T. Asayama, Y. Moriguchi, S. Agari, M. Onishi, *J. Am. Chem. Soc.* **2007**, *129*, 14160-14161;
- (b) Y. Arikawa, N. Matsumoto, T. Asayama, K. Umakoshi, M. Onishi, *Dalton Trans.* **2011**, *40*, 2148-2150;
- (c) Y. Arikawa, M. Onishi, *Coord. Chem. Rev.* **2012**, *256*, 468-478;
- (d) C. J. White, A. L. Speelman, C. Kupper, S. Demeshko, F. Meyer, J. P. Shanahan, E. E. Alp, M. Hu, J. Zhao, N. Lehnert, *J. Am. Chem. Soc.* **2018**, *140*, 2562-2574;
- (e) C. Van Stappen, N. Lehnert, *Inorg. Chem.* **2018**, *57*, 4252-4269.
- [5] Y. Arikawa, Y. Otsubo, H. Fujino, S. Horiuchi, E. Sakuda, K. Umakoshi, *J. Am. Chem. Soc.* **2018**, *140*, 842-847.
- [6] Y. Arikawa, A. Ikeda, N. Matsumoto, K. Umakoshi, *Dalton Trans.* **2013**, *42*, 11626-11631.
- [7] Y.-H. Lo, T.-H. Wang, C.-Y. Lee, Y.-H. Feng, *Organometallics* **2012**, *31*, 6887-6899.
- [8] A. García-Fernández, J. Díez, Á. Manteca, J. Sánchez, M. P. Gamasa, E. Lastra, *Polyhedron* **2008**, *27*, 1214-1228.
- [9] (a) Y. Arikawa, T. Nakamura, T. Higashi, S. Horiuchi, E. Sakuda, K. Umakoshi, *Eur. J. Inorg. Chem.* **2017**, *2017*, 881-884;
- (b) T. P. Brewster, W. Ding, N. D. Schley, N. Hazari, V. S. Batista, R. H. Crabtree, *Inorg. Chem.* **2011**, *50*, 11938-11946;
- (c) L. Vandenburg, M. R. Buck, D. A. Freedman, *Inorg. Chem.* **2008**, *47*, 9134-9136.
- [10] K. Matsumoto, T. Matsumoto, M. Kawano, H. Ohnuki, Y. Shichi, T. Nishide, T. Sato, *J. Am. Chem. Soc.* **1996**, *118*, 3597-3609.
- [11] F. E. Fernández, M. C. Puerta, P. Valerga, *Inorg. Chem.* **2013**, *52*, 4396-4410.
- [12] E. Rüba, C. Gemel, C. Slugovc, K. Mereiter, R. Schmid, K. Kirchner, *Organometallics* **1999**, *18*, 2275-2280.
- [13] (a) Í. Ferrer, X. Fontrodona, M. Rodríguez, I. Romero, *Dalton Trans.* **2016**, *45*, 3163-3174;
- (b) M. M. R. Choudhuri, R. J. Crutchley, *Inorg. Chem.* **2013**, *52*, 14404-14410;
- (c) R. Stephan, M. Somnath, B.-B. Jordi, P. Josefina, L. Antoni, *Eur. J. Inorg. Chem.* **2013**, *2013*, 232-240;
- (d) A. A. Rachford, J. L. Petersen, J. J. Rack, *Inorg. Chem.* **2005**, *44*, 8065-8075;

- (e) C. Sens, M. Rodríguez, I. Romero, A. Llobet, T. Parella, B. P. Sullivan, J. Benet-Buchholz, *Inorg. Chem.* **2003**, *42*, 2040-2048;
- (f) M. Sano, H. Taube, *Inorg. Chem.* **1994**, *33*, 705-709.
- [14] (a) F. Roncaroli, L. M. Baraldo, L. D. Slep, J. A. Olabe, *Inorg. Chem.* **2002**, *41*, 1930-1939;
- (b) J. L. Bear, J. Wellhoff, G. Royal, E. V. Caemelbecke, S. Eapen, K. M. Kadish, *Inorg. Chem.* **2001**, *40*, 2282-2286.
- [15] Data Collection and Processing Software, Rigaku Corporation (1998-2015), Tokyo 196-8666, Japan.
- [16] Rigaku (1998), Rigaku Corporation, Tokyo, 196-8666, Japan.
- [17] Crystal Structure Analysis Package, Rigaku Corporation (2000-2018), Tokyo 196-8666, Japan.

**Table 1.** N-O stretching frequencies ( $\text{cm}^{-1}$ ) and selected geometric parameters ( $\text{\AA}$ ,  $^\circ$ ) for **1 - 6**

	$\nu_{\text{NO}}$	Ru-NO	N-O	Ru-N-O
<b>1</b> [6]	1883	1.813(8)	1.145(12)	166.1(9)
<b>2</b>	1876	1.7625(18)	1.139(2)	169.57(17)
<b>3a</b>	1878	1.764(3)	1.145(4) <sup>c</sup>	163.1(3)
<b>4</b>	1483	1.968(6) 1.978(6)	1.240(7)	122.2(5) 120.8(5)
<b>5</b>	1888	1.767(6)	1.139(9)	161.0(6)
<b>6</b>	1914	1.763(4) 1.750(6)	1.140(5) 1.156(8)	168.3(4) 169.4(6)

**Table 2.** Crystallographic data for [ $\{\text{TpRu}(\text{NCS})\}\{\text{TpRu}(\text{NO})\}(\mu\text{-Cl})(\mu\text{-pz})$ ] (**2**), [ $\{(\text{TpRu}(\text{NO}))(\text{TpRu})(\mu\text{-Cl})(\mu\text{-pz})\}_2(\mu\text{-S}_2)\}(\text{BF}_4)_2$ ] (**3a**), [ $(\text{TpRu})_2(\mu\text{-NO})(\mu\text{-pz})(\mu\text{-S}_2)$ ] (**4**), [ $\{\text{TpRu}(\text{dmsO-}\kappa\text{S})\}\{\text{TpRu}(\text{NO})\}(\mu\text{-Cl})(\mu\text{-pz})\}\text{BF}_4$ ] (**5**), and [ $\{\text{TpRu}(\text{dmsO-}\kappa\text{O})\}\{\text{TpRu}(\text{NO})\}(\mu\text{-Cl})(\mu\text{-pz})\}(\text{NO}_3)_2$ ] (**6**)

	<b>2</b> ·2EtOH	<b>3a</b> ·4MeCN·2H <sub>2</sub> O	<b>4</b> ·CH <sub>2</sub> Cl <sub>2</sub>
formula	C <sub>26</sub> H <sub>35</sub> B <sub>2</sub> ClN <sub>16</sub> O <sub>3</sub> Ru <sub>2</sub> S C <sub>22</sub> H <sub>25</sub> B <sub>2</sub> Cl <sub>2</sub> N <sub>15</sub> ORu <sub>2</sub> S <sub>2</sub>	C <sub>50</sub> H <sub>62</sub> B <sub>6</sub> Cl <sub>2</sub> F <sub>8</sub> N <sub>34</sub> O <sub>4</sub> Ru <sub>4</sub> S <sub>2</sub>	
fw	910.94	1959.42	874.33
cryst system	monoclinic	monoclinic	orthorhombic
space group	<i>P</i> 2 <sub>1</sub> / <i>n</i> (No. 14)	<i>P</i> 2 <sub>1</sub> / <i>c</i> (No. 14)	<i>Pna</i> 2 <sub>1</sub> (No. 33)
color of crystal	dark-green	green	red-purple
crystal size (mm)	0.17 x 0.15 x 0.05	0.26 x 0.17 x 0.10	0.20 x 0.02 x 0.01
<i>a</i> (Å)	12.620(2)	13.2287(17)	14.643(3)
<i>b</i> (Å)	14.980(3)	15.194(2)	13.619(2)
<i>c</i> (Å)	18.820(4)	18.993(3)	15.944(3)
$\alpha$ (deg)	90	90	90
$\beta$ (deg)	92.620(3)	90.063(2)	90
$\gamma$ (deg)	90	90	90
<i>V</i> (Å <sup>3</sup> )	3554.2(12)	3817.5(9)	3179.6(10)
<i>Z</i>	4	2	4
$\rho_{\text{calc}}$ (g cm <sup>-3</sup> )	1.702	1.704	1.826
$\mu$ (cm <sup>-1</sup> )	10.396	9.873	12.970
2 $\theta_{\text{max}}$ (deg)	54.9	55.0	55.0
no. of all reflns collected	28987	30777	25330
no. of unique reflns	8114	8716	7238
<i>R</i> <sub>int</sub>	0.0273	0.0423	0.0446
no. of obsd reflns <sup>a</sup>	6895	7522	6632
no. of parameters	464	493	416
<i>R</i> <sub>1</sub> <sup>a, b</sup>	0.0257	0.0458	0.0438
w <i>R</i> <sub>2</sub> (all data) <sup>c</sup>	0.0628	0.1096	0.0860
GOF (all data) <sup>d</sup>	1.059	1.099	1.076
CCDC numbers	1881800	1881801	1881802

<sup>a</sup>  $I > 2\sigma(I)$ . <sup>b</sup>  $R_1 = \sum ||Fo| - |Fc|| / \sum |Fo|$ . <sup>c</sup>  $wR_2 = \{\sum w(Fo^2 - Fc^2)^2 / \sum w(Fo^2)^2\}^{1/2}$ .

<sup>d</sup>  $\text{GOF} = [\sum w(Fo^2 - Fc^2)^2 / (No - Np)]^{1/2}$ , where *No* and *Np* denote the number of data and parameters.

**Table 2.** (Continued)

	5·MeOH	6·H <sub>2</sub> O
formula	C <sub>24</sub> H <sub>33</sub> B <sub>3</sub> ClF <sub>4</sub> N <sub>15</sub> O <sub>3</sub> Ru <sub>2</sub> S	C <sub>23</sub> H <sub>31</sub> B <sub>2</sub> ClN <sub>17</sub> O <sub>9</sub> Ru <sub>2</sub> S
fw	957.70	980.88
cryst system	monoclinic	monoclinic
space group	<i>P</i> 2 <sub>1</sub> / <i>n</i> (No. 14)	<i>P</i> 2 <sub>1</sub> / <i>c</i> (No. 14)
color of crystal	dark-green	red
crystal size (mm)	0.14 x 0.06 x 0.02	0.15 x 0.13 x 0.04
<i>a</i> (Å)	17.446(4)	32.967(4)
<i>b</i> (Å)	12.490(2)	18.0125(19)
<i>c</i> (Å)	17.891(4)	14.8009(17)
$\alpha$ (deg)	90	90
$\beta$ (deg)	108.394(3)	100.5806(17)
$\gamma$ (deg)	90	90
<i>V</i> (Å <sup>3</sup> )	3699.4(13)	8639.6(17)
<i>Z</i>	4	8
$\rho_{\text{calc}}$ (g cm <sup>-3</sup> )	1.719	1.508
$\mu$ (cm <sup>-1</sup> )	10.170	8.718
2 $\theta_{\text{max}}$ (deg)	54.9	62.9
no. of all reflns collected	30210	80465
no. of unique reflns	8441	25627
<i>R</i> <sub>int</sub>	0.0537	0.0490
no. of obsd reflns <sup>a</sup>	6481	18733
no. of parameters	468	971
<i>R</i> <sub>1</sub> <sup>a, b</sup>	0.0812	0.0754
w <i>R</i> <sub>2</sub> (all data) <sup>c</sup>	0.1048	0.1001
GOF (all data) <sup>d</sup>	1.115	1.054
CCDC numbers	1881803	1881804

<sup>a</sup>  $I > 2\sigma(I)$ . <sup>b</sup>  $R_1 = \Sigma ||Fo| - |Fc|| / \Sigma |Fo|$ . <sup>c</sup>  $wR_2 = \{\Sigma w(Fo^2 - Fc^2)^2 / \Sigma w(Fo^2)^2\}^{1/2}$ .

<sup>d</sup> GOF =  $[\{\Sigma w(Fo^2 - Fc^2)^2\} / (No - Np)]^{1/2}$ , where *No* and *Np* denote the number of data and parameters.